# Isoprene and monoterpene emissions in Australia: comparison of a multi-layer canopy model with MEGAN and with atmospheric concentration observations

Kathryn M. Emmerson[1], Martin E. Cope[1], Ian E. Galbally[1], Sunhee Lee[1], Peter F. Nelson[2]

[1]CSIRO Climate Research Centre, PMB1, Aspendale, VIC 3195, Australia
[2]Environmental Sciences, Macquarie University, NSW 2109, Australia

*Correspondence to*: Kathryn Emmerson (kathryn.emmerson@csiro.au)

## 1.    The Australian Biogenic Canopy and Grass Emissions Model (ABCGEM)

The ABCGEM model was developed 15 years ago at CSIRO to provide a spatially and temporally resolved interactive biogenic emission inventory for the C-CTM. ABCGEM treats the emissions of reactive organic carbon from a full tree canopy (for which in-canopy gradients of temperature and radiation are parameterised) and from pasture and grasses. Cases which fall between these extremes (i.e. sparse canopy with an under-layer of pasture) are treated as a linear combination of the two separate approaches.

The emission rate, ER ($\mu$g-C m$^{-2}$ h$^{-1}$) within the model from either tree canopy or grasses is a function of the fraction of the model grid cell occupied by tree canopy or grass, F, the total leaf biomass $B_m$ (g m$^{-2}$), and plant genus-specific emission rate Q ($\mu$g-C g$^{-2}$ h$^{-1}$).

$$ER = F \times B_m \times Q \tag{1}$$

$B_m$ is the total dry weight of leaves extending from the ground to the canopy/grass height, $h_C$ per unit area of ground. Both $B_m$ and F relate to the projected leaf area index, LAI (m$^2$ m$^{-2}$). Thus:

$$F = 1 - exp^{(-0.5 \times LAI)} \tag{2}$$

$$B_m = LAI \times LMA \tag{3}$$

Where LMA is the leaf mass per unit area (g m$^{-2}$). $B_m$ changes with the seasonal variation in LAI and the relationship in equation 3. LMA is 100 g m$^{-2}$ for trees, consistent with studies in National Parks within the Sydney GMR (Wright et al., 2002), and 250 g m$^{-2}$ for grass. This higher ratio for grass is based on local measurements of pasture grass by Kirstine et al. (1998), but is more than expected by the global database of plant traits (Kattge et al., 2011). It does allow for very low values of $LAI_G$ in ABCGEM, but until mapped $B_m$ becomes available, equation 3 is a source of uncertainty. The leaf level emission rates, Q, are calculated for isoprene and monoterpenes in the tree canopy model (section 1.1), and for the grass model (section 1.3).

### 1.1.   The tree canopy model

The tree canopy is divided into 10 vertical layers each of which has a specified height and LAI. The vertical distribution of LAI follows a triangular distribution (Lamb et al., 1993), with the peak LAI occurring at two-thirds of the canopy height and drops to zero at one-third of canopy height (i.e. the trunk). The canopy model takes input conditions of solar radiation and air temperature and computes in-canopy gradients of temperature and solar radiation, for sunlit and shaded leaves. Layer-specific biogenic fluxes are then generated using the Guenther algorithms and a species-specific emission factor, normalised to 30 °C and 1000 $\mu$mol m$^{-2}$ s$^{-1}$.

### 1.1.1 Temperature Function

The temperature within the 10-layer canopy is assumed to change in proportion to the cumulative leaf area index, $LAI_C$, summed from the top down. During daylight hours, the leaf level temperature, $T_{leaf}$ of the $i^{th}$ layer, is approximated by the LAI-weighted interpolation of the leaf temperature between the top of the canopy, $T_h$ and the temperature at the canopy base, $T_{base}$.

$$5 \quad T_{leaf}^i = T_h + (LAI_C / LAI)[T_{base} - T_h] \tag{4}$$

where LAI is the projected canopy leaf area index per unit area of ground extending from the ground to $h_C$, the canopy height. ABCGEM does not consider the energy balance within the canopy, instead assuming that $T_{base}$ does not vary significantly diurnally, for a densely shaded canopy with no horizontal temperature advection. The 24-hour average temperature is used for $T_{base}$. At night, a height-based linear interpolation replaces equation 4.

10 The temperature correction function for isoprene emissions, $C_T$ for each layer is given by equation 5 (Guenther et al., 1991):

$$C_T = \frac{\exp\frac{C_{T1}(T_{leaf} - T_S)}{R\, T_S\, T_{leaf}}}{1 + \exp\frac{C_{T2}(T_{leaf} - T_M)}{R\, T_S\, T_{leaf}}} \tag{5}$$

where R = 8.314 J K-1 mol-1 , $C_{T1}$ = 95,000 J mol-1, $C_{T2}$ = 230,000 J mol-1 , $T_M$ = 314 °K and $T_S$ = 303 °K is the standard temperature. Whilst the above parameters have changed little since Guenther et al. (1991), there is evidence that temperature and light responses differ among plant species and can even vary among shade- and sun- adapted leaves within canopy and
15 individual trees (Sharkey et al., 1996; Harley et al., 1997).

### 1.1.2 Radiation Function

Leaf-level emissions require the specification of the incident photosynthetically active radiation (PAR) through the canopy. The attenuation of radiation through the canopy is determined using a relationship developed by Zhang et al., (2001).

$$PAR_{shade} = R_{diff}\, e^{(-0.65 LAI_i^{1.5})} + 0.07 R_{dir}(1.1 - 0.1 LAI_C)e^{-\cos\theta} \tag{6}$$

20 where $PAR_{shade}$ is the PAR flux on the shaded leaves, $R_{diff}$ is the diffuse radiation at the top of the canopy, $R_{dir}$ is the direct radiation at the top of the canopy, and θ is the solar zenith angle. The PAR flux incident on the sunlit leaves is given by Norman (1982):

$$PAR_{sun} = R_{dir} \cos\delta / \cos\theta + PAR_{shade} \tag{7}$$

where δ is the mean angle between the direction of leaves and the sun's rays.
25 In the case of isoprene emissions, the radiation correction function $C_L$ is given by equation 8 (Guenther et al., 1993):

$$C_L = \frac{\alpha\, C_{L1}\, L}{\sqrt{1 + \alpha^2\, L^2}} \tag{8}$$

Where α = 0.0027 and $C_{L1}$ = 1.066 and L is the PAR flux (μmol m-2 s-1), calculated as above for both $PAR_{sun}$ and $PAR_{shade}$.

A simple canopy radiation attenuation model is used to calculate the fraction of leaf area that is sunlit and shaded. Following Norman (1982), the cumulative leaf area index (integrated from the top of the canopy downwards) of sunlit leaves, $LAI_{sun,}$ and
30 shaded leaves, $LAI_{shade}$, is given by equations 9 and 10.

$$LAI_{sun} = 2\cos\theta \left[1 - e^{(-0.5\, LAI_C / \cos\theta)}\right] \tag{9}$$

and $LAI_{shade} = LAI_C - LAI_{sun}$ (10)

### 1.1.3 Layer-specific emission algorithm for isoprene

Following the prescription of the layer-specific leaf temperature, solar radiation flux and LAI, a leaf-level emission rate $Q_{leaf}$ for the $i^{th}$ layer, is calculated using equation 11. Note equation 11 only applies to isoprene:

$$Q_{leaf}^i = C_T^i[C_{Lsun}^i LAI_{sun}^i + C_{Lshade}^i LAI_{shade}^i] \tag{11}$$

5    $Q_{leaf}^i$ is dimensionless. The emission rate is an LAI-weighted sum of the flux from the sunlit and shaded areas of the leaf.

### 1.1.4 Layer-specific emission algorithm for monoterpenes

Monoterpene emissions are regarded as temperature dependent in ABCGEM. This dependence is related to the vapour pressure and transport resistance along the diffusion path, associated with volatilization of the monoterpenes out of leaf storage organs (Tingey et al., 1980; Simon et al., 1994). The emission response to temperature in the $i^{th}$ layer has an exponential increase with

10    temperature, described using the formula by Tingey et al. (1980):

$$Q_{leaf}^i = \exp\left(\beta(T_{leaf} - T_S)\right) \times LAI_i \tag{12}$$

Where $Q_{leaf}^i$ is the monoterpene emission rate at the leaf temperature $T_{leaf}$ within each layer, i, $T_S$ is the standard temperature (303 K) and $\beta$ ($K^{-1}$) is an empirical coefficient set to 0.09 $K^{-1}$ for all monoterpenes and plant species (Guenther et al., 1993). $LAI_i$ is the leaf area index (sunlit and shaded) within layer i.

15    ### 1.1.5 Tree canopy total emission rate

The tree canopy total emission rate, Q ($\mu$g-C $g^{-1}$ $h^{-1}$), is obtained by scaling the leaf-level emission rate for either isoprene or monoterpenes, by the projected LAI. For our 10-layer canopy,

$$Q = EF_S \sum_{i=1}^{10-layer}[Q_{leaf}^i]/LAI \tag{13}$$

Where $EF_S$ is the species-specific normalised emission factor ($\mu$g-C $g^{-1}$ $h^{-1}$). $EF_S$ is modified according to the ambient

20    conditions of temperature and PAR (isoprene only) on leaves within each layer.

### 1.3 The grass model

The grass emission model is that of Kirstine et al. (1998). They measured a mean normalised VOC emission factor of 0.4 $\mu$g-C $g^{-1}$ $h^{-1}$ over a fertilized but ungrazed pasture site ~100 km from Melbourne in south east Australia. Kirstine et al. (1998) observed pasture biomass varying between 2300 g $m^{-2}$ during the growing season to 940 g $m^{-2}$ at the end of summer. This

25    yielded a seasonal average $B_m$ of 1600 g $m^{-2}$. Such pasture would typically be cut for fodder and as such the leaf biomass measured is higher than expected for grass. The prefix to equation 14 takes the emission factor and average $B_m$ into account, and the total VOC emission flux over grass ($\mu$g-C $m^{-2}$ $h^{-1}$) becomes Q in equation 1:

$$Q = 9.01 \times 10^{-7} PAR^3 (2.46 \times 10^{-3} T_l^2 - 6.22 \times 10^{-7} T_l^4 - 1) \tag{14}$$

where $T_l$ is the leaf temperature and PAR = $PAR_{sun}$ + $PAR_{shade}$

30    Q is then scaled to ambient conditions using $B_m$ applicable to the current model grid cell as per equation 1. In contrast to eucalypt VOC emissions, oxygenated species such as methanol (13 %), ethanol (18 %), acetaldehyde (14 %) and acetone (16 %) comprise the dominant VOC species emitted from pastures and grasses. Isoprene and monoterpenes represent 5 % each of the total VOC emitted from grass.

## 2. CSIRO CTM model setup

The C-CTM is set up with parameters and input data described in Table 1.

**Table 1 Input datasets and characteristics of ABCGEM and MEGAN modelling**

|  | **ABCGEM (this work)** | **MEGAN (Emmerson et al., 2016)** |
| --- | --- | --- |
| Meteorology, including temperature and PAR | CCAM | CCAM |
| Chemistry scheme | Carbon Bond 5 | Carbon Bond 5 |
| Anthropogenic emissions | GMR inventory (DECCW, 2007) | GMR inventory (DECCW, 2007) |
| LAI | Monthly grids for trees and grass (Lu et al., 2003) | Monthly MODIS files, for current and previous monthly LAI. |
| Plant Functional Type, PFT | 2 classes: trees and grass | 16 PFTs from IGBP dataset (Belward et al., 1999) |
| Emission factors, EFs | Canopy: fixed at 25 $\mu$g-C g$^{-1}$ h$^{-1}$ for isoprene and 2.5 $\mu$g-C g$^{-1}$ h$^{-1}$ for monoterpenes. Grass: fixed at 0.02 $\mu$g-C g$^{-1}$ h$^{-1}$ for both isoprene and monoterpenes. | Mapped emission factors for 10 species, including isoprene and 7 monoterpene species; fixed values dependent on PFTs for the other 137 species |
| No. of layers in canopy model | 10 (8 above trunk) | 5 |
| Considers energy balance? | No | Yes |

### 2.1 The LAI input datasets

The LAI parameter influences isoprene and monoterpene emission rates, impacting on the temperature and PAR throughout the canopy (equations 4 to 13), the biomass density (equation 3) and, for ABCGEM, the fractional coverage (equation 2). Figure 1 shows the ABCGEM LAI tree and grass products. Whilst the spatial distribution in LAI protrudes into the sea due to the coarse resolution of the parent dataset, the associated land use for these locations (ocean) used in the model ensure there are no biogenic emissions. Tree canopies have much higher LAIs than grass. However the grass LAI varies with season, whilst the tree LAI does not (evergreen species). However due to negligible grass emission factors, these additional grass LAI values are considered 'empty' and do not contribute to the modelled emission rates of isoprene or monoterpenes.
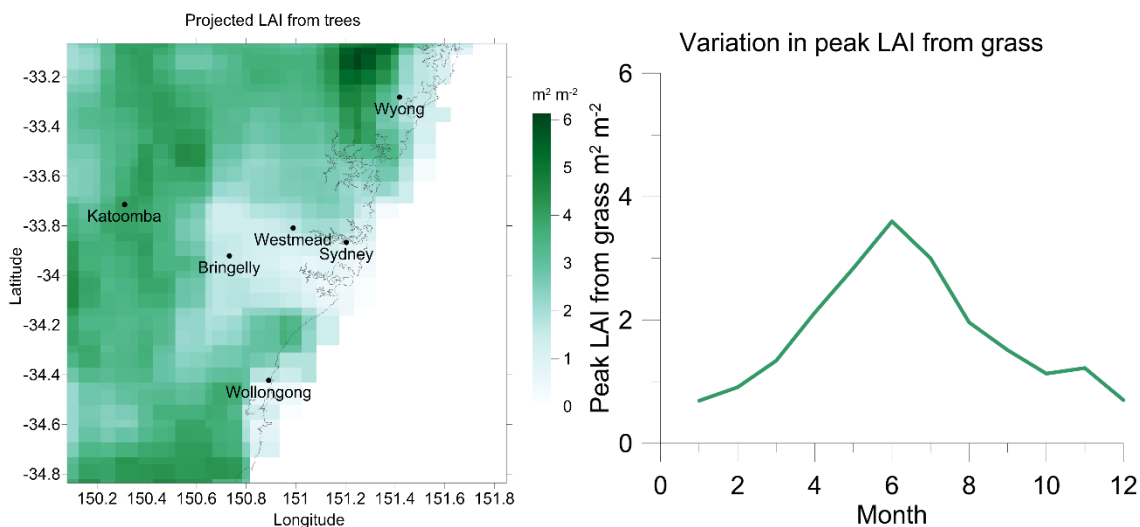
**Figure 1 Projected leaf area index for (left) trees and (right) grass within the inner domain for ABCGEM.**

## 2.2 MEGAN emission rates

The equations for the MEGAN emission rates are repeated here from Emmerson et al. (2016). They relate to the implementation of MEGANv2.1 within the C-CTM.

MEGANv2.1 provides two approaches for estimating emission factors. The first is to use the 16 plant functional type (PFT) distributions and the global average PFT specific emission factors listed in Table 2 of Guenther et al. (2012). In this case the emission rate, R ($\mu$g m$^{-2}$ hr$^{-1}$) of species i in any grid box, will be sensitive to the PFT distributions used for the MEGAN simulation (equation 15):

$$R_i = \sum_{j=1}^{nPFT}\left(EF_{ij} \times \gamma_{ij} \times \chi_j\right) \qquad (15)$$

where $EF_{ij}$ is the emission factor ($\mu$g m$^{-2}$ hr$^{-1}$) of species i under standard conditions for PFT j with fractional grid box areal coverage $\chi_j$. The emission activity factor $\gamma_{ij}$ (dimensionless) accounts for emission control processes and uses the following variables to drive the canopy model: compound class, response to light and temperature, leaf age, soil moisture, $CO_2$ and LAI. The second approach is to use MEGAN global emission factor maps, which are based on plant type composition and plant type specific emission factors. In this case, the MEGAN simulation uses PFTs to define the canopy environment characteristics and to define the fractional grid box areal coverage, but the results are not as sensitive to the PFT data used. The emission rate, R for species i in a given grid cell, xy is (equation 16):

$$R_i = EF_{i,\,xy} \sum_{j=1}^{nPFT}\left(\gamma_{ij} \times \chi_j\right) \qquad (16)$$

This study uses both approaches, the latter approach for 10 species where emission factor maps are available, and the former approach for all other species.

## 3. ABCGEM emission estimate uncertainty analysis

The uncertainty analysis of these BVOC emission estimates proceeds via the ABCGEM emission algorithm, using the principles in the Guide to Expression of Uncertainty in Measurement and the law of propagation of uncertainty (JCGM, 2008) also known as the error propagation equation (Berrington and Robinson, 1992; Harris, 2003). All uncertainties in this analysis are expanded uncertainties with a coverage factor k = 2. The associated level of confidence of the uncertainty interval is typically 95%.

The equation for propagation of uncertainty for the function $x = f(u, v, \dots)$ is:

$$\sigma_x^2 = \sigma_u^2 \left(\frac{\partial x}{\partial u}\right)^2 + \sigma_v^2 \left(\frac{\partial x}{\partial v}\right)^2 + \qquad 2\sigma_{uv}^2 \left(\frac{\partial x}{\partial u}\right)^2 \left(\frac{\partial x}{\partial v}\right)^2 \dots \qquad (17)$$

In this equation and subsequent uncertainty interpretations, variances are represented as population values. In the calculations the experimentally determined variances are used. We assume that all uncertainties evaluated here are uncorrelated, except where explicitly stated.

## 3.1 ABCGEM emission uncertainty

The basic equation for BVOC emission estimates includes the following terms:

$B_m$      total dry mass of leaves extending from the ground to the canopy/grass height per unit area of ground, (g m$^{-2}$)

$h_C$      canopy/grass height (m)

| | | |
|---|---|---|
| F | fraction of the model grid cell occupied by tree canopy or grass (dimensionless) | |
| LAI | leaf area index, $(m^2\ m^{-2})$ | |
| LMA | leaf mass per unit leaf area, $(g\ m^{-2})$ | |
| PAR | photosynthetic active radiation | |
| T | temperature (K) | |
| ER | emission rate, $(\mu g\text{-}C\ m^{-2}\ h^{-1})$ | |
| Q | plant genus-specific emission rate $(\mu g\text{-}C\ g^{-2}\ h^{-1})$ | |
| EF | plant genus-specific emission factor | |
| SZA | solar zenith angle | |

With subscripts

| | |
|---|---|
| T | tree |
| G | grass |
| S | plant genus |

The emission rate within the model from either tree canopy or grasses is a function of the fraction of the model grid cell occupied by tree canopy or grass (equation 2), the total leaf biomass (equation 3), and plant genus-specific emission rate (equations 13 and 14).

$$Q = f(T, PAR, SZA, LAI, EF_s) \hspace{2cm} (18)$$

Because the grass emissions are <1% of total, for the uncertainty analysis, grass emissions can be neglected. The SZA comes into the determination of fraction of shaded and sunlit leaves and is considered here to be a second order effect. The uncertainties are presented in Table 2. The uncertainty in LAI is determined by the maximum difference in slope between the LAIs from the comparison of the MEGAN and the Lu et al. (2003) data set. The uncertainty in EFs in equation 18 is derived from the comparison of the MEGAN and ABCGEM EFs at LAI interval 2 – 3 in Figure 2 of the main paper. The uncertainty in the fractional coverage of a plant genus across the landscape $F_T$ is based on a change of plant genus for 50% of the land area from Eucalypts to either Acacia or Pittosporum (Emmerson et al. 2016). Such an uncertainty is based on the inadequate mapping of tree genera across the GMR area.

The following uncertainties are presented in Table 2: $\sigma_{ER}$ , $\sigma_{LAI}$ , $\sigma_T$ , $\sigma_{PAR}$ , $\sigma_{EF_S}$, $\sigma_{F_T}$

These are substituted in equation (6) to give the combined relative uncertainty.

$$\sigma_{ER}^2/ER^2 = \sigma_{LAI}^2/LAI^2 + \sigma_T^2/T^2 + \sigma_{PAR}^2/PAR^2 + \sigma_{EF_S}^2/EF_S^2 + \sigma_{F_T}^2/F_T^2 \hspace{1cm} (19)$$

The estimate is of the uncertainty in the isoprene emissions averaged over the GMR domain for the period of a field campaign and as stated earlier represent 95% confidence limits. It is apparent from combining the relative variances from the uncertainties in Table 2, that the LAI, Emission Factor, EFs, and landscape coverage are the major sources of uncertainty in ABCGEM. The expanded combined relative uncertainty 0.82 (95% CL). In fact because the relative uncertainty is approaching 1, the uncertainties are probably asymmetric and expressing the result as a relative uncertainty of approximately a factor of 2 is probably more realistic. The result of the analysis indicates that plant genera BVOC emissions, plant genera distribution and leaf area index are the key areas requiring more information to improve this ABCGEM modelling.

**Table 2 Uncertainty analysis for campaign based average emission**

| Term | Variable | Relative expanded uncertainty (σ) | Combined expanded relative uncertainty | Reference |
|---|---|---|---|---|
| 1 Temperature | T (deg C) | 0.1 | | Cope et al. (2014) |
| 2 Photosynthetic active radiation | PAR | 0.1 | | estimate |
| 3 Leaf area index | LAI | 0.4 | | This study |
| 4 Emission factor of plant genus | EFs | 0.5 | | This study |
| 5 Fractional cover of plant genus | $F_T$ | 0.5 | 0.82 | This study |

## 4 Differences between ABCGEM and MEGAN temperature activity functions

As ABCGEM was developed 15 years ago independently of MEGAN, there are some subtle differences in the way the calculated emission rates respond to temperature. ABCGEM uses 303 K as the standard temperature for both isoprene

5 (equation 5) and monoterpene (equation 12) calculations. In MEGAN v2.1, a standard temperature of 297 K is used for light dependent compounds, whilst 303.15 K is used for light independent compounds. There is also a difference in the value of β in equation 12; ABCGEM uses 0.09, whereas MEGAN uses 0.1.

The monoterpene emission rates from the SPS1 period are split into daytime (6:30 – 19:30 hours) and night time hours, and sorted by the LAI parameter in Figure 2. The daytime emission rates are approximately 2.5 times greater than the night time

10 emission rates in all models. However the gradient in ABCGEM/AML monoterpene emission rates are approximately 3 times greater than the MEGAN emission rates. In MEGAN the impact of the temperature activity function is reduced because monoterpenes exhibit varying degrees of light dependency.
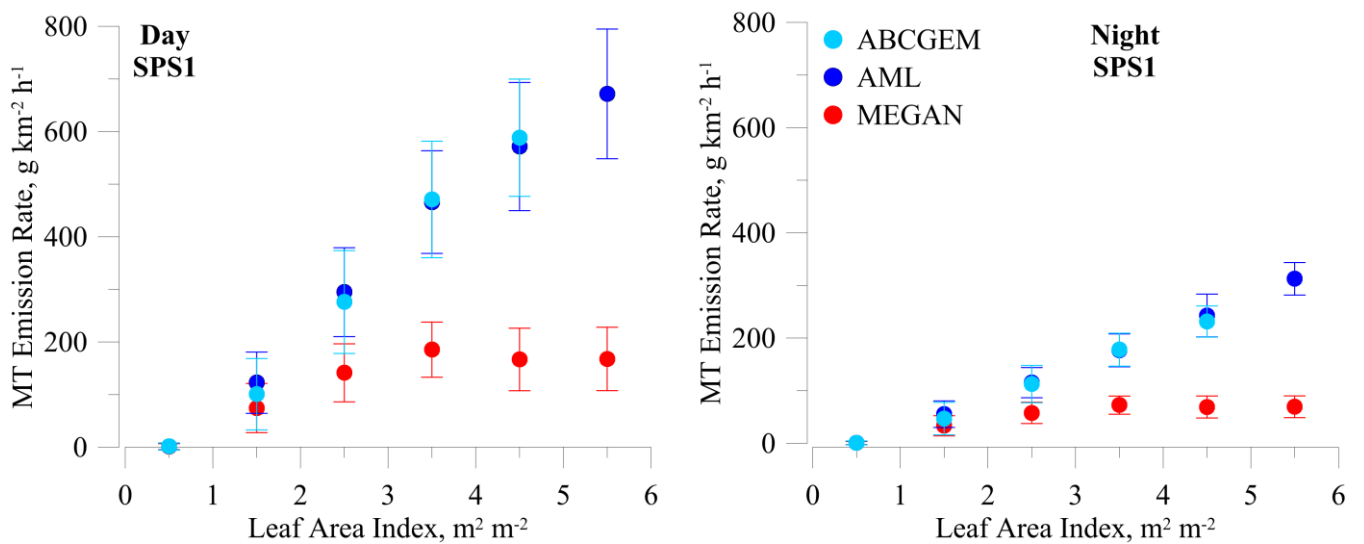
15 **Figure 2 Impacts on average monoterpene (MT) emission rates in all models during SPS1 campaign split by (left) daytime and (right) night-time.**

## 5  Results for the autumnal SPS2 campaign

SPS2 occurred during April/May of 2012, which is autumn in the southern hemisphere. Conditions were cooler than the other field campaigns studied, and the LAI dataset for the ABCGEM scheme at this time of year exhibited much more growth than the MEGAN LAI dataset. This led to higher isoprene predictions during SPS2 for ABCGEM compared with MEGAN, which needed reasoning.

### 5.1  Emission factors with LAI during SPS2

Figure 3 shows how the isoprene and monoterpene emission factors between ABCGEM and MEGAN differ when compared with the respective scheme's LAI for the SPS2 period (tree LAI only for ABCGEM). The MEGAN isoprene emission factors plateau after the peak at LAI of 3 - 4 $m^2$ $m^{-2}$, whilst the ABCGEM isoprene emission factors keep increasing. The ABCGEM LAI has slightly more land grid cells at higher LAI values than the MEGAN LAI. The ABCGEM LAI peaks at 6.1 $m^2$ $m^{-2}$, whilst the MEGAN autumn LAI dataset here has a maximum of 5 $m^2$ $m^{-2}$. Note that these higher 5 - 6 $m^2$ $m^{-2}$ bin contain less than 1% of the land area and thus the emission factor points have been removed. 30% of the land area in MEGAN is in LAI bins 2 - 3 $m^2$ $m^{-2}$.
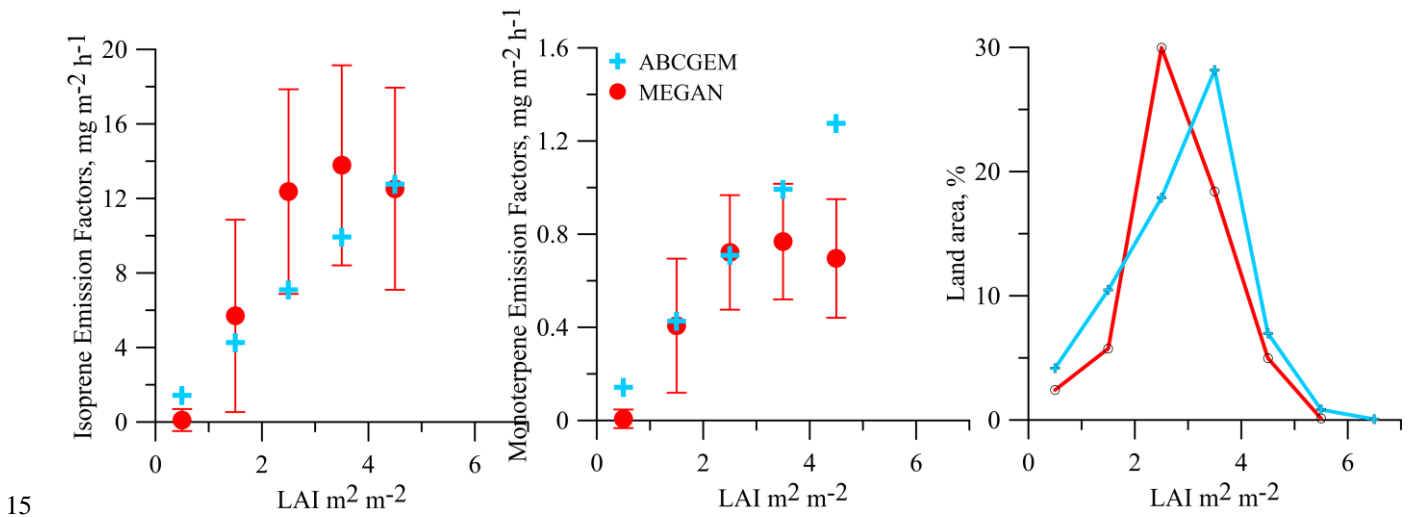
**Figure 3 Scatter plot of the canopy isoprene (left) and monoterpene (middle) emission factors across the Sydney grid with LAI for ABCGEM and MEGAN during April/May. Note y-axes are not the same. (Right) percentage of land area taken up by each LAI bin in April/May (SPS2). Error bars represent ± 1 standard deviation.**

### 5.2 Spatial distributions of emission rates during SPS2

Figure 4 shows maps of the grid cell average emission rates for MEGAN and ABCGEM for the timing of the SPS2 field campaign, followed by the differences in between MEGAN and ABCGEM. Compared with the summer period of SPS1, the autumnal SPS2 isoprene emission rates are a factor of ~8 lower in MEGAN compared with SPS1 and a factor of ~3 lower for monoterpenes in ABCGEM. The emission rates for SPS2 show similar patterns as were seen in the SPS1 distributions. These relate to the higher ABCGEM isoprene emission within the Sydney urban and suburban areas than MEGAN, and the higher MEGAN monoterpenes to the immediate south west of Sydney.
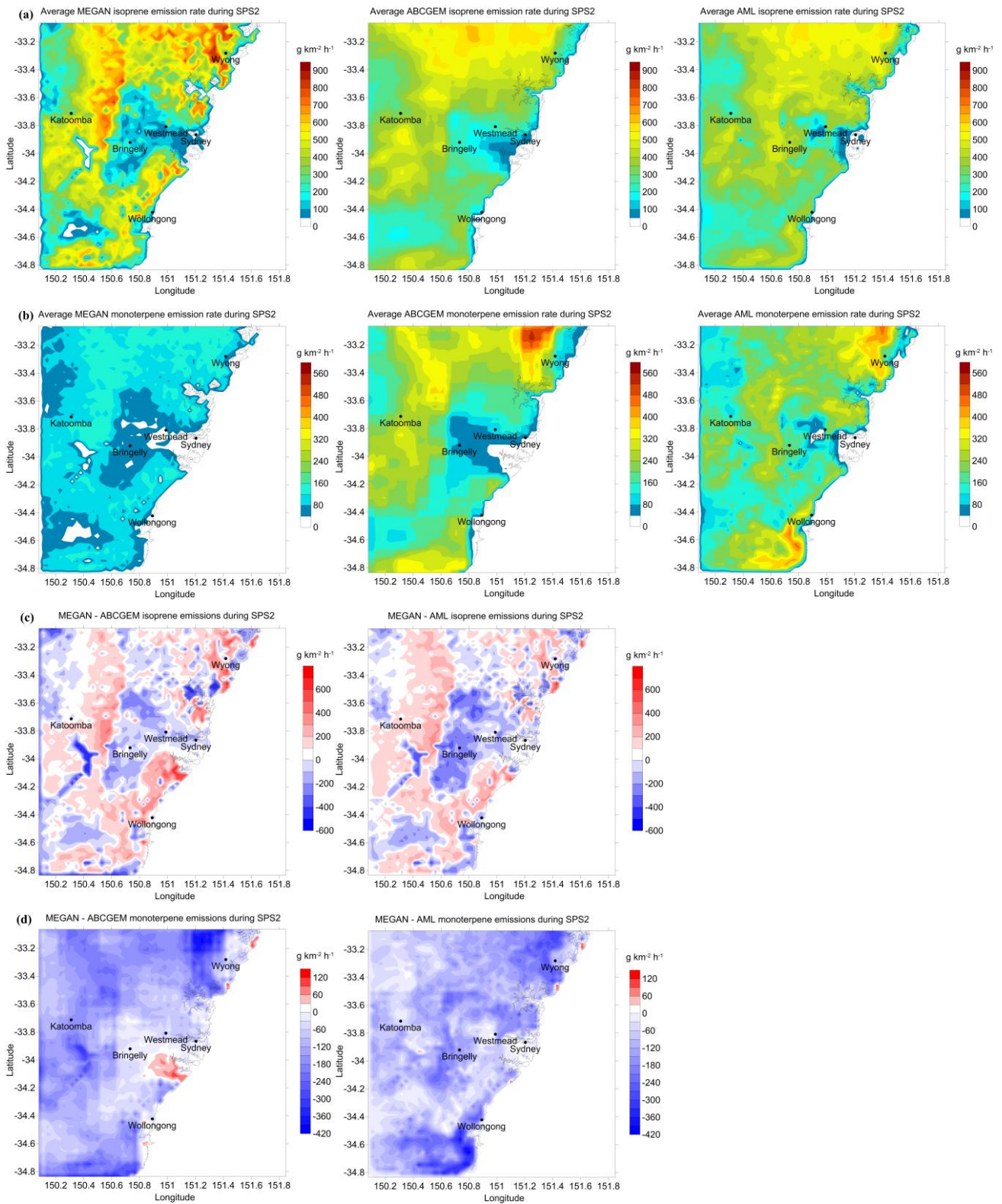
**Figure 4 Spatial distributions of grid cell average emission rates for (a) isoprene (b) monoterpenes, and the differences between MEGAN with ABCGEM or AML emission rates for (c) isoprene and (d) monoterpenes for the SPS2 campaign. Note: scales are unalike for isoprene and monoterpenes.**

## 6    Wind rose analyses

Measurements of wind speed and direction were taken at the field campaign sites, and provide information on the meteorological conditions experienced. Wollongong and Randwick sites are both close to the coast and yet exhibit different diurnal cycles in isoprene concentrations (both measured and modelled). The Wollongong isoprene diurnal profile is as expected, with high isoprene at noon. The Randwick isoprene diurnal profile is not expected, with an isoprene peak before 9am, which then tails away to low concentrations during the daylight hours. Campaign average wind roses are plotted of the observations in Figure 5, and show where the influences of each field site are coming from, e.g. Bringelly from the south west, and SPS1 from the north west; both regions of high isoprene emission factors. However these wind roses do not show the average diurnal variation required for Wollongong and Randwick, as it is suspected that fresh onshore air masses must be reaching Randwick during daylight hours.
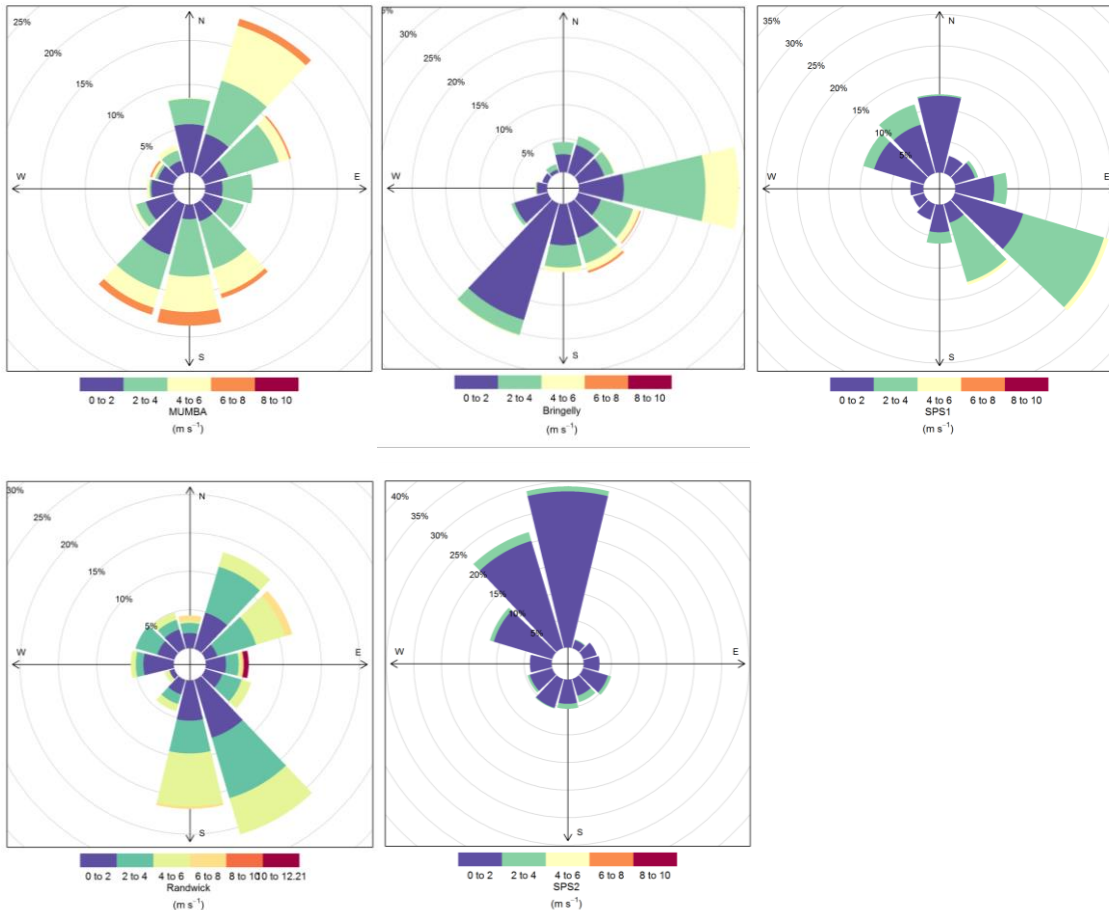
**Figure 5 Observed wind roses for each field campaign.**

The position of Wollongong and Randwick are shown in Figure 6 with the campaign average wind rose aligned due north. This demonstrates that the MUMBA site at Wollongong will still receive the bulk of its air mases after transport over land. The Randwick site has some stronger easterlies which will be fresh sea air. The timings of the wind mass changes are better observed by splitting the data into hourly wind roses.
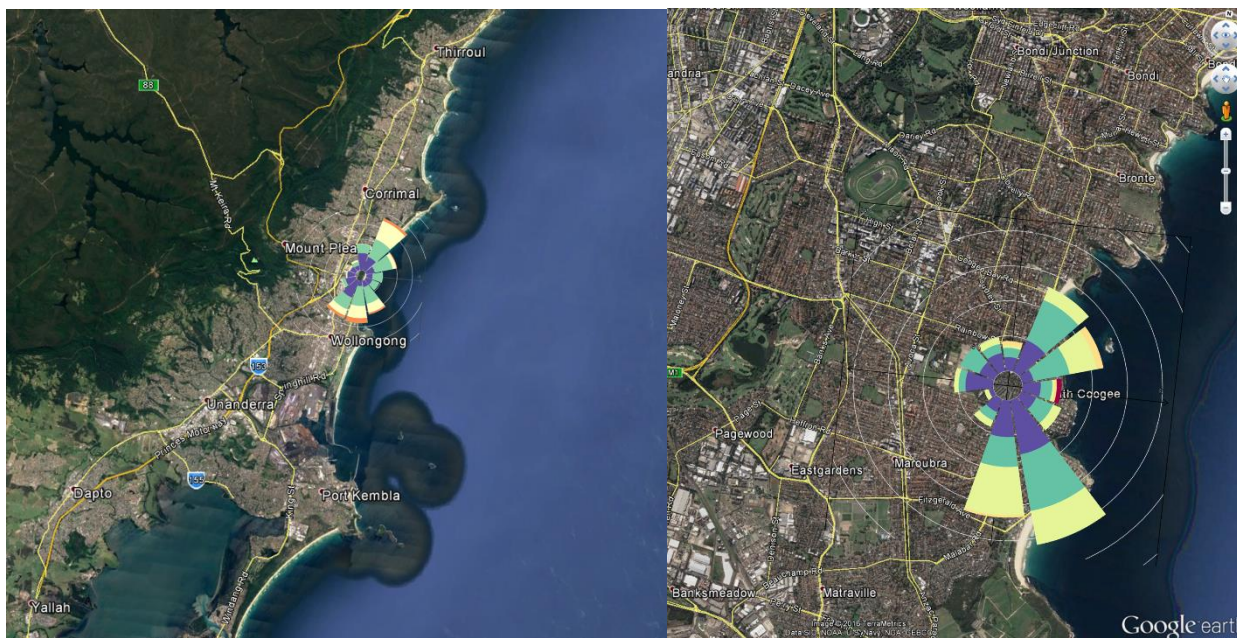
**Figure 6 Maps to demonstrate average wind direction at MUBA (left) and Randwick (right) field sites.**

The MUMBA wind roses (Figure 7) show winds blowing from the south west until 8am when they start to swing from the south east until noon and then from the north east in the early afternoon until 7pm. Winds then become lighter in strength.

5   The Randwick wind roses (Figure 8) show a different pattern. There are gaps in the measurements, however before 9am there are generally light winds. The wind speed picks up after 11am blowing from the south east and easterly directions, with speeds of up to 12 m s$^{-1}$ from the east between 2 and 4 pm. After 5pm, there are stronger winds from the north east. The position of Randwick near the coast suggests that there would be few biogenic air masses reaching the site after 11am. The meteorology explains the difference in diurnal concentrations of isoprene observed at Wollongong and Randwick. The monoterpene diurnal

10   profiles are not affected as fast reaction times during the day mean their concentrations only build up overnight when wind speeds are calmer.
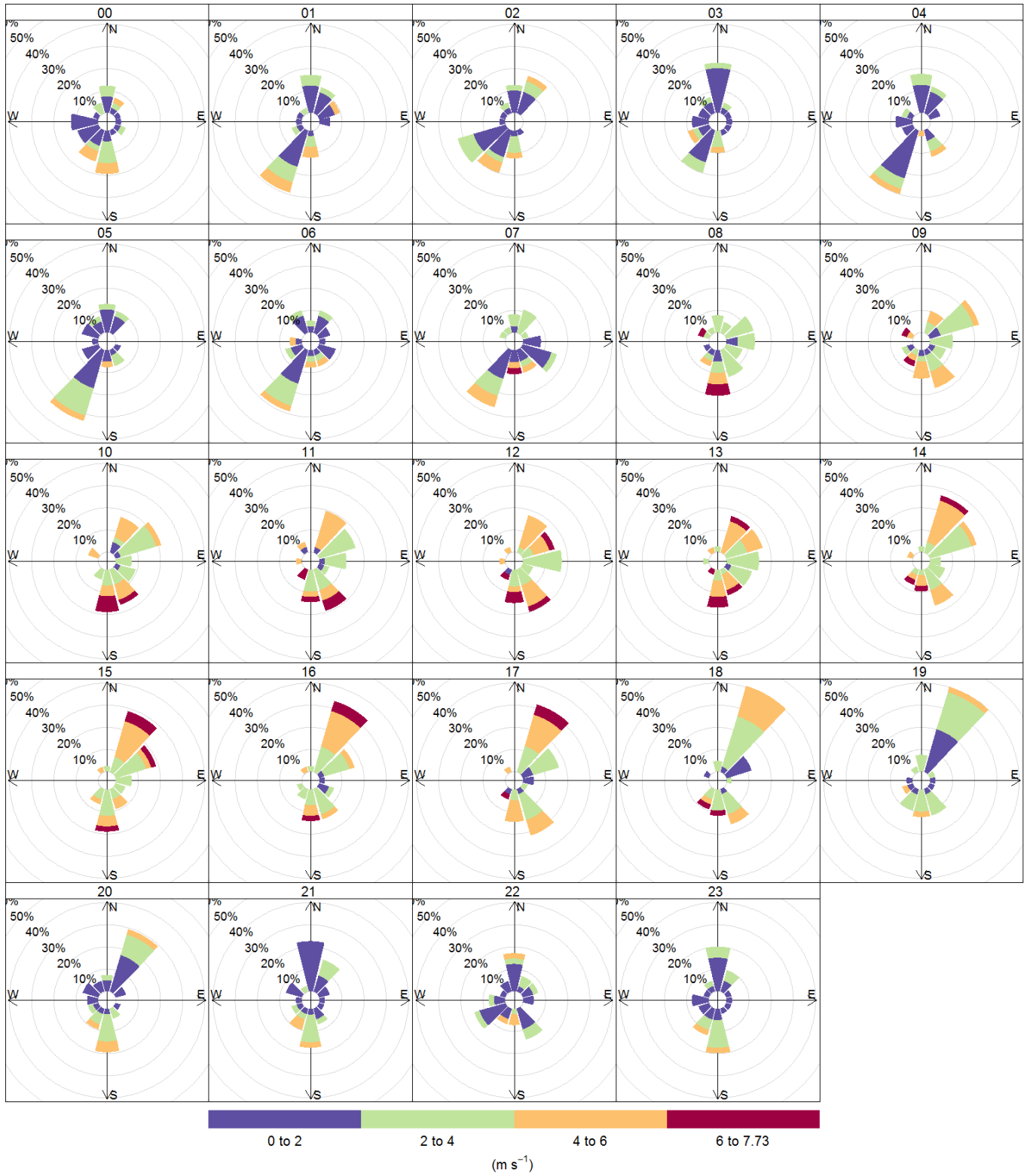
**Figure 7. Wind roses, plotted each hour, averaged for the MUMBA observations.**
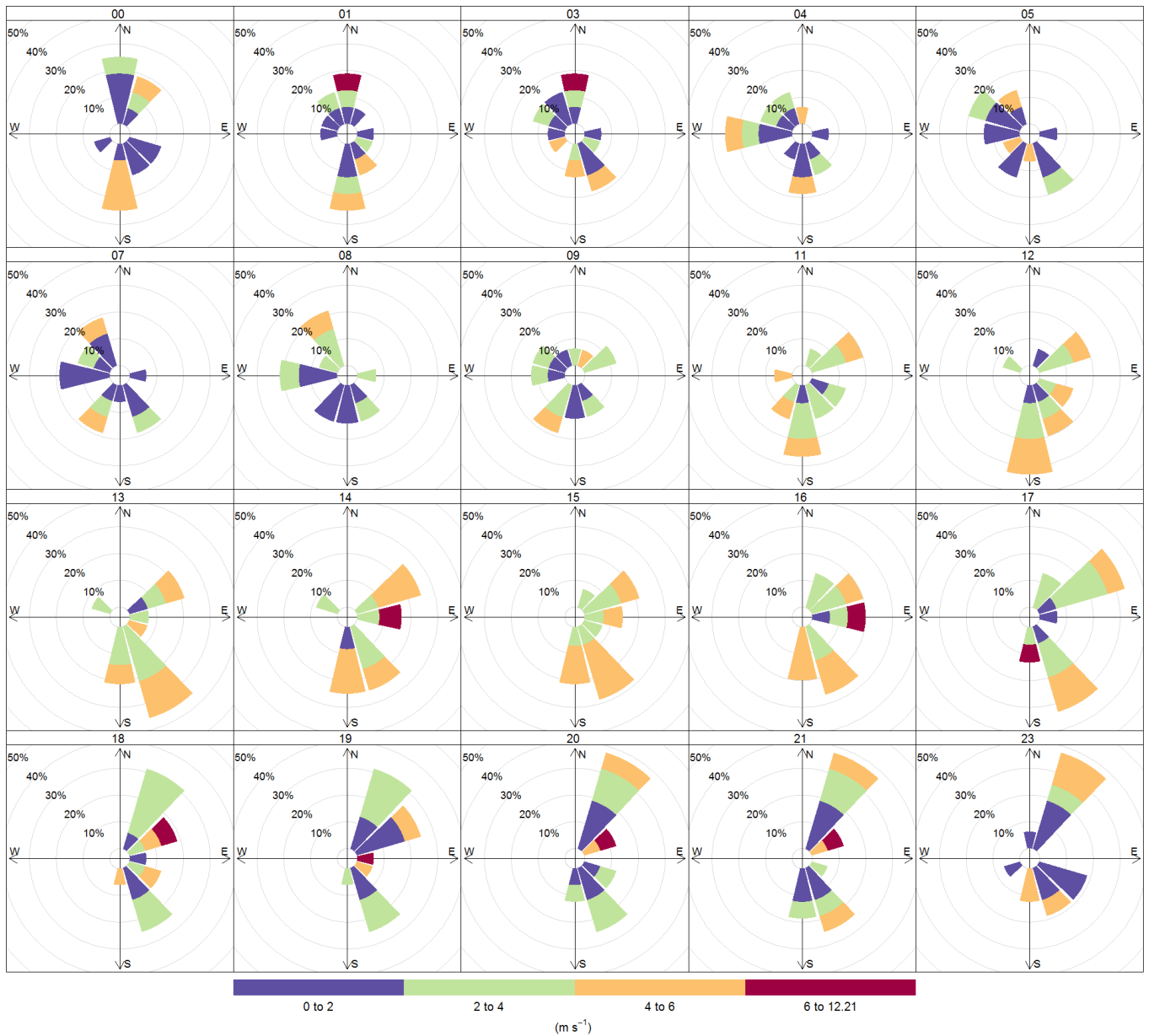
**Figure 8 Wind roses, plotted each hour, averaged for the Randwick observations. Note, there are gaps in the observations at 2am, 6am, 10am and 10pm.**

## 6    References

Berrington, P. R., and Robinson, D. K.: Data reduction and error propagation for the physical sciences, McGraw-Hill, Boston, 328 pp., 1992.

Guenther, A. B., Monson, R. K., and Fall, R.: Isoprene and Monoterpene Emission Rate Variability - Observations with Eucalyptus and Emission Rate Algorithm Development, J Geophys Res-Atmos, 96, 10799-10808, Doi 10.1029/91jd00960, 1991.

Guenther, A. B., Zimmerman, P. R., Harley, P. C., Monson, R. K., and Fall, R.: Isoprene and Monoterpene Emission Rate Variability - Model Evaluations and Sensitivity Analyses, J Geophys Res-Atmos, 98, 12609-12617, Doi 10.1029/93jd00527, 1993.

Harley, P., Guenther, A., and Zimmerman, P.: Environmental controls over isoprene emission in deciduous oak canopies, Tree Physiol, 17, 705-714, 1997.

Harris, D. C.: Quantitative Chemical Analysis, 6th Edition ed., W.H. Freeman and Co, New York, 2003.

JCGM: JCGM 100: 2008 Evaluation of measurement data. Guide to the expression of uncertainty in measurement. , BIPM, Sevres, France, 2008.

Kattge, J., Diaz, S., Lavorel, S., Prentice, C., Leadley, P., Bonisch, G., Garnier, E., Westoby, M., Reich, P. B., Wright, I. J., Cornelissen, J. H. C., Violle, C., Harrison, S. P., van Bodegom, P. M., Reichstein, M., Enquist, B. J., Soudzilovskaia, N. A., Ackerly, D. D., Anand, M., Atkin, O., Bahn, M., Baker, T. R., Baldocchi, D., Bekker, R., Blanco, C. C., Blonder, B., Bond, W. J., Bradstock, R., Bunker, D. E., Casanoves, F., Cavender-Bares, J., Chambers, J. Q., Chapin, F. S., Chave, J., Coomes, D., Cornwell, W. K., Craine, J. M., Dobrin, B. H., Duarte, L., Durka, W., Elser, J., Esser, G., Estiarte, M., Fagan, W. F., Fang, J., Fernandez-Mendez, F., Fidelis, A., Finegan, B., Flores, O., Ford, H., Frank, D., Freschet, G. T., Fyllas, N. M., Gallagher, R. V., Green, W. A., Gutierrez, A. G., Hickler, T., Higgins, S. I., Hodgson, J. G., Jalili, A., Jansen, S., Joly, C. A., Kerkhoff, A. J., Kirkup, D., Kitajima, K., Kleyer, M., Klotz, S., Knops, J. M. H., Kramer, K., Kuhn, I., Kurokawa, H., Laughlin, D., Lee, T. D., Leishman, M., Lens, F., Lenz, T., Lewis, S. L., Lloyd, J., Llusia, J., Louault, F., Ma, S., Mahecha, M. D., Manning, P., Massad, T., Medlyn, B. E., Messier, J., Moles, A. T., Muller, S. C., Nadrowski, K., Naeem, S., Niinemets, U., Nollert, S., Nuske, A., Ogaya, R., Oleksyn, J., Onipchenko, V. G., Onoda, Y., Ordonez, J., Overbeck, G., Ozinga, W. A., Patino, S., Paula, S., Pausas, J. G., Penuelas, J., Phillips, O. L., Pillar, V., Poorter, H., Poorter, L., Poschlod, P., Prinzing, A., Proulx, R., Rammig, A., Reinsch, S., Reu, B., Sack, L., Salgado-Negre, B., Sardans, J., Shiodera, S., Shipley, B., Siefert, A., Sosinski, E., Soussana, J. F., Swaine, E., Swenson, N., Thompson, K., Thornton, P., Waldram, M., Weiher, E., White, M., White, S., Wright, S. J., Yguel, B., Zaehle, S., Zanne, A. E., and Wirth, C.: TRY - a global database of plant traits, Global Change Biol, 17, 2905-2935, 10.1111/j.1365-2486.2011.02451.x, 2011.

Kirstine, W., Galbally, I., Ye, Y. R., and Hooper, M.: Emissions of volatile organic compounds (primarily oxygenated species) from pasture, J Geophys Res-Atmos, 103, 10605-10619, Doi 10.1029/97jd03753, 1998.

Lamb, B., Gay, D., Westberg, H., and Pierce, T.: A Biogenic Hydrocarbon Emission Inventory for the USA Using a Simple Forest Canopy Model, Atmos Environ a-Gen, 27, 1673-1690, Doi 10.1016/0960-1686(93)90230-V, 1993.

Norman, J. M. I. J. E.: Simulation of microclimates, in: Biometeorology in Integrated Pest Management., edited by: Hatfield, J. L., and Thomason, I., Academic Press, New York,, 65-99., 1982.

Sharkey, T. D., Singsaas, E. L., Vanderveer, P. J., and Geron, C.: Field measurements of isoprene emission from trees in response to temperature and light, Tree Physiol, 16, 649-654, 1996.

Simon, V., Clement, B., Riba, M. L., and Torres, L.: The Landes Experiment - Monoterpenes Emitted from the Maritime Pine, J Geophys Res-Atmos, 99, 16501-16510, Doi 10.1029/94jd00785, 1994.

Tingey, D. T., Manning, M., Grothaus, L. C., and Burns, W. F.: Influence of Light and Temperature on Monoterpene Emission Rates from Slash Pine, Plant Physiol, 65, 797-801, DOI 10.1104/pp.65.5.797, 1980.

Wright, I. J., Westoby, M., and Reich, P. B.: Convergence towards higher leaf mass per area in dry and nutrient-poor habitats has different consequences for leaf life span, J Ecol, 90, 534-543, DOI 10.1046/j.1365-2745.2002.00689.x, 2002.

Zhang, L. M., Moran, M. D., and Brook, J. R.: A comparison of models to estimate in-canopy photosynthetically active radiation and their influence on canopy stomatal resistance, Atmos Environ, 35, 4463-4470, Doi 10.1016/S1352-2310(01)00225-4, 2001.